

Review

The Application of Pyrolysis Biochar Obtained from Waste Rapeseed Cake to Remove Copper from Industrial Wastewater: An Overview

Krzysztof Mazurek ^{*ID}, Sebastian Drużyński ^{ID}, Urszula Kiełkowska ^{ID}, Adriana Wróbel-Kaszanek, Bartłomiej Igliński ^{*ID} and Marcin Cichosz ^{ID}

Faculty of Chemistry, Nicolaus Copernicus University in Toruń, Gagarina 7, 87-100 Toruń, Poland; sebdru@umk.pl (S.D.); ulak@chem.umk.pl (U.K.); adriana@umk.pl (A.W.-K.); chemik@chem.umk.pl (M.C.)
* Correspondence: k.mazurek@umk.pl (K.M.); iglinski@umk.pl (B.I.); Tel.: +48-56-6114309 (K.M.)

Abstract: Pyrolysis is a thermochemical technology for converting biomass into energy and chemical products consisting of bio-gas, bio-oil, and biochar. Several parameters influence the process efficiency and properties of pyrolysis products. These include the type of biomass, biomass preliminary preparation, gaseous atmosphere, final temperature, heating rate, and process time. This manuscript provides a general summary of the properties of the pyrolytic products of waste rapeseed cake, with particular emphasis on the sorption properties of biochar. Biochar, produced by the pyrolysis process of biomass, is emerging as a powerful tool for carbon sequestration, reducing greenhouse gas emissions, and purifying water from contaminants such as potentially toxic elements and antibiotics. The review found that the biochar obtained as a result of pyrolysis of chemically modified waste rapeseed cake is characterised by its excellent sorption properties. The obtained sorbents are characterised by sorption capacity relative to the copper(II) ion, ranging from 40 mg·g⁻¹ to 100 mg·g⁻¹, according to the pyrolysis conditions and chemical modification method. The purified pyrolysis gas obtained in the high-temperature process can be used to generate heat and energy. Bio-oil, with its significant combustion heat of 36 MJ·kg⁻¹, can be a source of environmentally friendly green biofuel.

Keywords: biomass; rapeseed cake; pyrolysis; bio-gas; bio-oil; biochar; removal; adsorption; copper



Citation: Mazurek, K.; Drużyński, S.; Kiełkowska, U.; Wróbel-Kaszanek, A.; Igliński, B.; Cichosz, M. The Application of Pyrolysis Biochar Obtained from Waste Rapeseed Cake to Remove Copper from Industrial Wastewater: An Overview. *Energies* **2024**, *17*, 498. <https://doi.org/10.3390/en17020498>

Academic Editor: Dimitrios Kalderis

Received: 19 December 2023

Revised: 5 January 2024

Accepted: 18 January 2024

Published: 19 January 2024



Copyright: © 2024 by the authors. Licensee MDPI, Basel, Switzerland. This article is an open access article distributed under the terms and conditions of the Creative Commons Attribution (CC BY) license (<https://creativecommons.org/licenses/by/4.0/>).

1. Introduction

Industrial activities are closely related to waste generation, which has a negative impact on the natural environment. The negative impact of anthropogenic pressure is intensified by demographic growth and rapid civilisation development. Therefore, among the main goals of all policy areas of European Union countries, as expressed in Directive 2008/98/EC, are activities favouring technological and equipment solutions aiming to reduce the amount of waste that is generated and regulate the waste management system [1–8].

The volume of the industrial production of sulphuric(VI) acid worldwide has been increasing for years. It is estimated that a total of approximately 279 million metric tons of monohydrate will be produced in 2024. This will constitute an increase of approximately 13% in the production volume in 2015 [9]. In Poland, the annual production of sulphuric(VI) acid has been fluctuating at around 1.5–2.0 million metric tons of monohydrate for many years. H₂SO₄ is produced in three types of industrial plants: metallurgical plants, sulphur plants, and wet catalysis plants. The type of installation determines the amount and type of waste that is generated [10–13].

Waste wash acids are produced in metallurgical installations. They are created at the purification stage of the process gas that is sent to sulphuric acid factories directly from the metallurgical unit. Process gas purification aims to remove impurities that may be harmful at further stages of sulphuric(VI) acid production using the contact method. The amount

and chemical composition of the wash acids that are produced depends on many factors. In the metallurgical unit, waste electrolytic acids are produced as a result of the electrolysis process. Waste electrolytic acids are characterised by a much higher acid concentration than wash acids. Table 1 shows sample concentrations of agents contaminating the acids in question [10–15].

Table 1. Characterisation of waste acids from the non-ferrous metals industry [11,15].

Compound	Content, ppm
Cu	1–300
Zn	2–100
As	2–1000
Fe	10–100

A commonly used method for managing and utilising waste acids is the process of chemical stabilisation of the contaminants contained in them, which involves their precipitation in the form of sparingly soluble compounds. The precipitated sediments can be deposited or recycled. However, this technological process poses many difficulties, primarily due to the diverse composition and variable properties of the waste. Therefore, attempts are being made to develop new, more technologically advantageous ways of separating valuable components from the wastewater in question [10–15].

The adsorption process is a well-known and widely used method in chemical technology. It is characterised by high universality, mainly due to the high adsorption capacity of the sorbents used, the simplicity of the technological process and its high neutrality to the natural environment [16–20]. Activated carbons are the most frequently used adsorbents in the treatment of industrial wastewater containing potentially toxic elements [21–27]. However, this type of commercial adsorbent is expensive, which limits their use in many industrial processes. The development of a cheap and effective sorbent for the adsorption of ions of potentially toxic elements may be an attractive solution for industry, but it constitutes a serious challenge for materials engineering. Biochar offers great promise in this aspect. It is characterised by a specific, well-developed surface and porous structure with many different functional groups and mineral components. It has a porous structure that is similar to the structure of activated carbon, thanks to which it can become an effective adsorbent for the removal of both inorganic and organic contaminants from water. Additionally, unlike activated carbon, biochar is a new type of adsorbent, with low cost and high efficiency. The technology used to produce activated carbon requires a relatively higher process temperature and an additional activation process. Biochar, on the other hand, is cheaper to produce and uses less energy. It can be obtained from waste biomass. Therefore, biochar is a renewable resource, and ideal for water purification technologies due to its economic and environmental benefits [28–36].

One of the types of biomass that can be used in this way is waste rapeseed cake. It is obtained in the oil production process by pressing and extracting rapeseed seeds. Rapeseed is one of the most important oil plants [37–40]. The total production of rapeseed in the world has been increasing for many years, reaching nearly 90 million metric tons in 2022 [41–43]. The world leaders in rapeseed production are the European Union (19.5 million metric tons), Canada (19 million metric tons), and China (14.7 million metric tons) [43]. The world production of rapeseed oil in 2022 was approximately 32 million metric tons [43]. The increase in rapeseed oil production is accompanied by a proportional increase in waste, and in the case of meal, annual global production reached 71 million metric tons [44]. Rapeseed is also widely used as a source of protein for food and industrial applications, in the pharmaceutical industry and as an ornament, owing to the variety of flower colours [45–47].

The properties and composition of waste rapeseed cake depend on the rapeseed species and the technology and process conditions used. It is a form of organic waste rich in carbon and oxygen. It is characterised by its relatively low nitrogen and hydrogen

content and trace sulphur content. Currently, this waste is most often used as an animal feed additive.

This article summarises and compares the methods used to modify waste rapeseed cake and the properties of the carbon materials obtained from it, with particular emphasis on sorption and separation properties relative to the copper(II) ion [48–50]. The importance and purposefulness of this study are justified by the fact that copper deposits are being depleted in the world, and the demand for this metal is increasing. The demand for copper is estimated to double in the next 20–30 years [51,52].

2. Methods of Modification of Waste Rapeseed Cake

The waste rapeseed cake used in this study came from Prem-Vit Sp. J. Inowrocław, Poland. The authors' preliminary study has shown that the pyrolysate obtained from waste rapeseed cake is characterised by unsatisfactory physicochemical and adsorption properties. The material obtained in the pyrolysis process at a temperature of 700 °C proved to be non-porous, with a specific surface area of 0.35 m²·g⁻¹. There are few functional groups on its surface, which is why it has relatively weak adsorption properties [48–50].

Therefore, in the process of obtaining biochar from waste rapeseed cake, it is necessary to chemically modify the charge for the pyrolysis furnace to improve the effectiveness of the stage of creating a porous structure. For this purpose, before undergoing pyrolysis, raw rapeseed cake was subjected to modification processes:

Biochar 1—rapeseed cake was impregnated with a 40% solution of ammonium peroxydisulfate [48].

Biochar 2—rapeseed cake was impregnated with a mixture of magnesium chloride and ammonium peroxydisulfate [49].

Biochar 3—rapeseed cake was impregnated with 3M potassium silicate solution [50].

The mixtures were then left for 72 h at room temperature so that excess water could evaporate. The raw materials prepared in this way were subjected to pyrolysis at a temperature of 700 °C. The detailed procedure for preparing the charge for the pyrolysis furnace is described in [48–50].

3. Characteristics of the Obtained Products

The experiments carried out on unimpregnated rapeseed cake showed that the temperature of the pyrolysis process affects the amount of gaseous, liquid, and solid products obtained in the process. The process temperature had the smallest effect on the amount of gas that was released. The efficiency of gas production ranged from 11% to 16% (*m/m*) in the temperature range from 300 °C to 700 °C. An analysis of the chemical composition of the pyrolysis gas showed that an increase in the process temperature reduces the amount of carbon oxide that is emitted, particularly carbon(IV) oxide. At the same time, as the temperature of the pyrolysis process increased, the amount of energetically valuable methane significantly increased [48–50].

During the pyrolysis process that occurred at 700 °C, a gas sample with a density of 1.499 kg·m⁻³ was obtained. The gas mixture was then subjected to quantitative analysis in the Orsat apparatus. The main component of the obtained gas is carbon(IV) oxide—56.7% (*v/v*). The remaining components are as follows: methane—34.4% (*v/v*); unsaturated hydrocarbons—1.8% (*v/v*); and carbon(II) oxide—0.4% (*v/v*). In the resulting gas mixture, no hydrogen was observed. The main reason for the formation of such significant amounts of carbon oxides in the gas mixture is the oxidation of organic substances such as cellulose, hemicellulose, and lignin [48–50].

Similar results were obtained by Ucar and Ozkan [53], who determined the composition of the pyrolysis gas obtained at 500 °C using gas chromatography. They determined the CO₂ content in the tested mixture to be 69% (*m/m*). In addition to carbon(IV) oxide, the main components of the gas they obtained were carbon(II) oxide, C₁, C₂–C₇, and some hydrogen sulphide. According to the authors, the formation of the H₂S was derived from the nature of rapeseed oil cake since it contained 0.88% (*m/m*) sulphur.

Considering the chemical composition of the gas, its combustion heat was calculated to be $1708 \text{ kJ}\cdot\text{m}^{-3}$. This value is low and cannot be compared with nitrogenous natural gas, whose calorific value is $28,000 \text{ kJ}\cdot\text{m}^{-3}$. The combustion heat of the obtained gas increases to $12,702 \text{ kJ}\cdot\text{m}^{-3}$ if carbon dioxide is excluded from the calculations. This value allows for the product to be used for energy purposes, but the obtained pyrolysis gas must be cleaned of carbon dioxide.

Biogas is purified and modified depending on its use. Typically, biogas is focused on producing heat and steam, generating electricity, vehicle fuel production, chemical production, and the injection of biogas into natural gas transmission networks. Most biogas purification technologies were adapted from known technologies for natural gas refinement. Currently, several basic methods are used for biogas treatment. These include the following technologies: physical absorption in water or solvents, chemical absorption, pressure absorption, membrane separation, and biological conversion [54–58].

The liquid phase production efficiency for the tested process ranged from 50% to 59% (m/m), depending on the temperature used. Ozcimen and Karaosmanoglu [59], who examined the liquid fraction obtained from the pyrolysis of waste rapeseed cake in detail, have shown that the bio-oil obtained in this fraction is a fuel with a density of $993 \text{ kg}\cdot\text{m}^{-3}$, which has a high heat combustion value of $36 \text{ MJ}\cdot\text{kg}^{-1}$ and is rich in carbon and oxygen. Additionally, the liquid fraction is characterised by low nitrogen, sulphur, and ash contents. According to the authors, the bio-oil obtained in the pyrolysis of waste rapeseed cake can be used as a raw material in the fractional distillation process to obtain gasoline, diesel oil or alternative products to fuel oil. The fuels produced in this way could be used, either directly or indirectly, as an addition to the conventional fuels obtained from crude oil.

The efficiency of obtaining biochar decreases with an increase in the temperature of the pyrolysis process and does not exceed 40% [48–50].

4. Physicochemical Characteristics of the Obtained Biochars

The results of the Brunauer–Emmett–Teller analysis of the specific surface area of the studied biochars are presented in Table 2 [48–50]. The presented data show that all the obtained sorbents belong to porous materials and are characterised by their relatively small specific surface area. Their pores have a small volume and relatively large diameters. While Biochar 1 has the largest specific surface area ($167 \text{ m}^2\cdot\text{g}^{-1}$), Biochar 2 has the smallest ($11.4 \text{ m}^2\cdot\text{g}^{-1}$). It should be emphasised, however, that the surface area of all three biochars is significantly larger than the surface area of the carbon material obtained from pure cake, which was $0.35 \text{ m}^2\cdot\text{g}^{-1}$. This means that attempts to modify the surface result in the creation of a porous structure in the pyrolysis of waste rapeseed cake. The substances that are used can dehydrate carbohydrate polymers, accelerating the release of volatile substances and creating open pores upon heating. The small specific surface area of Biochar 2 compared to the other two biochars is the result of the pores being blocked by the magnesium oxide crystals located on the surface [60–65]. These observations were previously reported by Li et al. [66]. The researchers obtained MgO-modified biochar from sugar cane harvest residues. They discovered that the coal's specific surface area decreased from $118 \text{ m}^2\cdot\text{g}^{-1}$ to $27 \text{ m}^2\cdot\text{g}^{-1}$ as the MgO content increased from 2% to 20%. Additionally, the diameter, volume, and sorption capacity of pores significantly increased.

Table 2. The surface area and pore properties of the studied biochars [48–50].

Material	ABET, $\text{m}^2\cdot\text{g}^{-1}$	Pore Size, nm	Pore Volume, $\text{cm}^3\cdot\text{g}^{-1}$
Biochar 1	167.0	1.9	0.08
Biochar 2	11.4	2.0	0.04
Biochar 3	150.1	13.4	0.50

The biochars produced by modifying rapeseed cake have a comparable surface area to other carbon materials of this type that are described in the literature. For comparison, the specific surface areas of biochars obtained by Wang et al. [67] at temperatures of 300–700 °C

from different precursors (peanut husk, mud, bamboo reed, etc.) ranged from 3.75 to 54.05 m²·g⁻¹.

Table 3 shows the results of the elemental analysis of carbon, hydrogen, and nitrogen in the obtained sorbents. The carbon content does not exceed 73%, and the nitrogen content is relatively high, above 4% [48–50]. The degree of charring, expressed as the hydrogen/carbon (H/C) molar ratio, according to the data in Table 3, indicates that the method used to modify waste rapeseed cake significantly affects its value. The observed H/C coefficients of 0.28 (Biochar 1) and 0.33 (Biochar 2) are similar to those obtained for commercially activated carbon. The low H/C molar ratios indicate that the biochars are highly carbonised and lack the typical organic residues found in rapeseed, such as proteins or lignocellulosic fibres [68]. They are also characterised by a relatively high nitrogen content (4.5–5.6%). The presence of nitrogen has a positive effect on the adsorption properties of biochars. It can form highly polar functional groups on the surface of biochar, making the surface more hydrophilic.

Table 3. Biochars CHN elemental analysis results [48–50].

Material	C, %	H, %	N, %	C/H
Biochar 1	63.3	1.5	5.6	0.28
Biochar 2	58.7	1.6	5.2	0.33
Biochar 3	72.6	2.6	4.5	0.43

The thermogravimetric analysis and differential thermal analysis of biochar samples were carried out in an air atmosphere at a flow of 100 cm³·min⁻¹, with a heating rate of 5 °C·min⁻¹. The results are summarised in Table 4 [48–50]. The tested samples were decomposed in three or four stages. In the first endothermic stage, the samples lost adsorption moisture. In the second stage, the least stable oxygen groups, i.e., carboxyl, hydroxyl, and lactone groups, decomposed, and this was accompanied by the further loss of adsorption water. At the third stage of exothermic decomposition, nitrogen-containing groups decomposed due to the destruction of the carbon skeleton of the sample. In the fourth step, the most thermally stable sulphur groups decomposed.

Table 4. TGA-DTA analysis results of biochars [48–50].

Step	Mass Loss, %	Energy Effect	Temperature Range, °C
Biochar 1			
1	3.2	Endothermic	31–48
2	7.3	Endothermic	48–196
3	59.1	Exothermic	196–519
4	12.5	Exothermic	519–1000
Biochar 2			
1	3.9	Endothermic	23–120
2	9.7	Endothermic	120–173
3	37.4	Exothermic	173–559
4	3.8	Exothermic	559–698
Biochar 3			
1	3.2	Endothermic	22–30
2	4.1	Endothermic	30–177
3	80.4	Exothermic	177–607

The scanning electron microscope images in Figure 1 show that the sorption materials that were obtained consist of irregularly shaped particles and grains of varying sizes that tend to agglomerate. There are also deep cracks or pores on the outer surface of the obtained biochar, which may be formed as a result of the removal of volatile organic matter during pyrolysis [48–50].

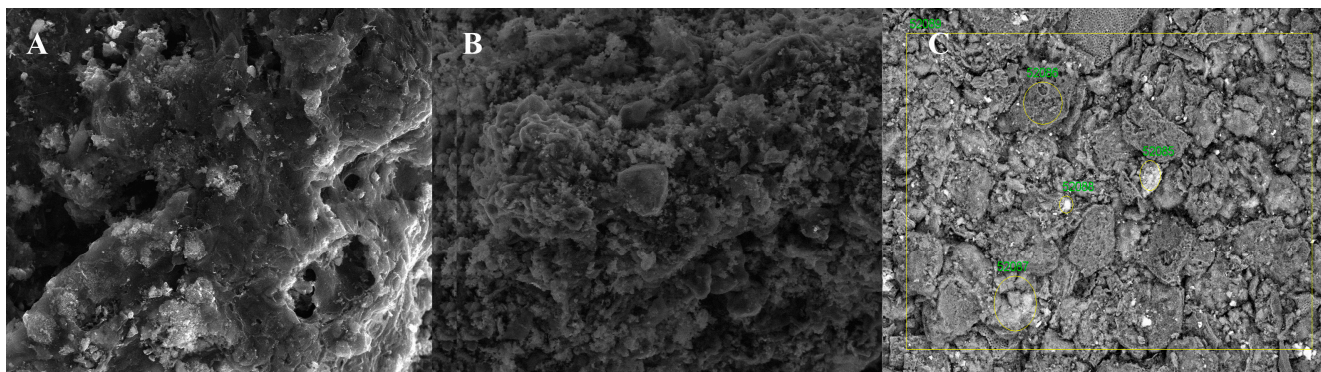


Figure 1. SEM images of obtained biochars: (A)—biochar 1; (B)—biochar 2; (C)—biochar 3.

Quantitative and qualitative analyses of the elemental composition of the obtained biochars conducted by the authors showed that these materials do not contain potentially toxic elements. This is extremely important in the context of their subsequent use in water purification processes. In addition to typical elements, such as C, N, O, and H, the authors only identified the presence of sodium, potassium, calcium, magnesium, aluminium, silicon, sulphur, phosphorus, chlorine, and iron. The content of the mentioned elements in unmodified biochar ranged from 0.3 to 3% [48–50].

5. Sorption Properties of the Obtained Biochars

The study showed that the carbon materials that are discussed in this paper have a relatively high affinity for copper(II) ion. The adsorption process for the proposed sorbents mainly depended on the contact time between the adsorbent and the adsorbate, the copper(II) cation concentration, the adsorption process temperature, the aqueous solution's pH, and the ratio of the solid phase to the liquid phase.

Figure 2 presents the results of tests focusing on how the pH of the solution affects the efficiency of the copper(II) ion adsorption process for the studied biochars. This parameter is crucial in ion adsorption processes with a solid adsorbent, including the proposed technological solution.

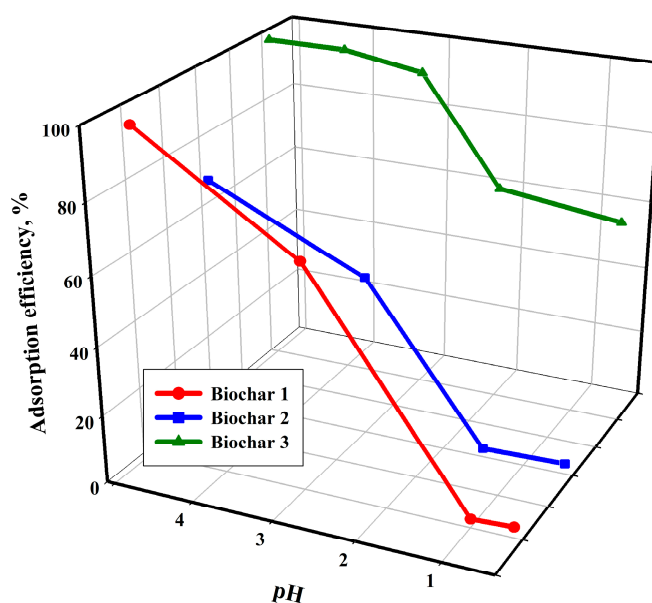


Figure 2. The adsorption process efficiency as a function of the aqueous solution pH ($T = 25\text{ }^{\circ}\text{C}$ (B1), $30\text{ }^{\circ}\text{C}$ (B2&B3); $t = 240$ (B1&B2), 120 (B3) min; $c = 100$ (B1), 200 (B2), 180 (B3) $\text{mg}\cdot\text{dm}^{-3}$; mass of adsorbent = 3.33 (B1), 1.67 (B2), 4 (B3) $\text{g}\cdot\text{dm}^{-3}$) [48–50].

Figure 2 presents experimental data indicating that the adsorption of copper(II) ions is less effective in strongly acidic environments compared to solutions with higher pH levels. At a low pH, functional groups on the sorbent surface become protonated, which reduces the adsorption of copper ions due to electrostatic repulsion between the cation and the positively charged sorbent surface. An increase in pH results in a change in the charge of the sorbent surface, leading to the generation of more negatively charged groups. In addition to the surface charge, the quality and quantity of ionic species present in the tested solution also influence the pH dependence of adsorption. It is important to remember that, at a pH of 5 or lower, copper(II) ion is present in the solution as Cu^{2+} . When the pH of the solution increases above 5, copper(II) hydroxo complexes— $\text{Cu}(\text{OH})^+$ are formed. $\text{Cu}(\text{OH})_2$ may be precipitated when the pH of the solution is above 6, dominating adsorption at a sufficiently high pH [69,70]. The described relationships are consistent with the results presented for other biochars [71–73]. Unlike the other two tested materials, Biochar 3 shows relatively good sorption properties in a low-pH environment. The cause of this phenomenon is attributed to the sorbent preparation method. As previously mentioned, the material underwent hydrothermal modification in a concentrated potassium hydroxide solution after the pyrolysis process. It can be assumed that the protons in the hydroxyl groups on the sorbent's surface were fully exchanged for potassium ions. The resulting bond between oxygen and the potassium ion is ionic and, therefore, when the Cu^{2+} ion solution is in contact with Biochar 3, the potassium ion is preferentially replaced by the Cu^{2+} ion.

The efficiency of the adsorption process is also influenced by the ratio of the solid phase to the liquid phase (S:L). This parameter determines the capacity of the adsorbent for the initial ion concentration in the solution. The experimental data presented in Figure 3 clearly indicate that a higher S:L ratio ($\text{g}\cdot\text{dm}^{-3}$) increases the obtained process efficiency. An increase in the mass of the adsorbent that was used provides more active sites for capturing or binding the copper ion. At the same time, the probability of collisions between the adsorbent and Cu^{2+} increases, improving the efficiency of cation removal from the tested solution [74].

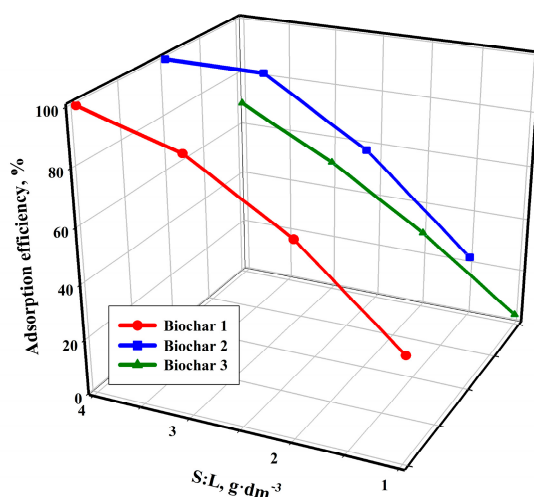


Figure 3. The adsorption process efficiency as a function of the solid-to-liquid ratio ($\text{g}\cdot\text{dm}^{-3}$) ($T = 25\text{ }^{\circ}\text{C}$ (B1), $30\text{ }^{\circ}\text{C}$ (B2), $20\text{ }^{\circ}\text{C}$ (B3); $t = 240$ (B1&B2), 120 (B3) min; $c = 100$ (B1&B3), 200 (B2) $\text{mg}\cdot\text{dm}^{-3}$; $\text{pH} = 5$) [48–50].

An analysis of the data presented in Figure 4 indicates that the efficiency of the adsorption process is also influenced by the increase in temperature. For all the tested sorbents, the lowest efficiency values were obtained at a temperature of $20\text{ }^{\circ}\text{C}$, while the highest were obtained at the highest tested temperature, i.e., $50\text{ }^{\circ}\text{C}$. The course of the points also shows that temperature affects the sorption on Biochar 3 to a much greater extent than

it affects the other two sorbents. The temperature-dependent increase in process efficiency indicates that the adsorption process of the copper(II) cation is endothermic. An increase in process temperature leads to greater pore penetration by the studied cation and the creation of new active sites. Additionally, the higher temperature affects the kinetic energy of Cu^{2+} , resulting in increased mobility and spontaneous adsorption. A higher temperature reduces the viscosity of the solution, which, in turn, increases the diffusion rates and adsorption efficiency [75–77].

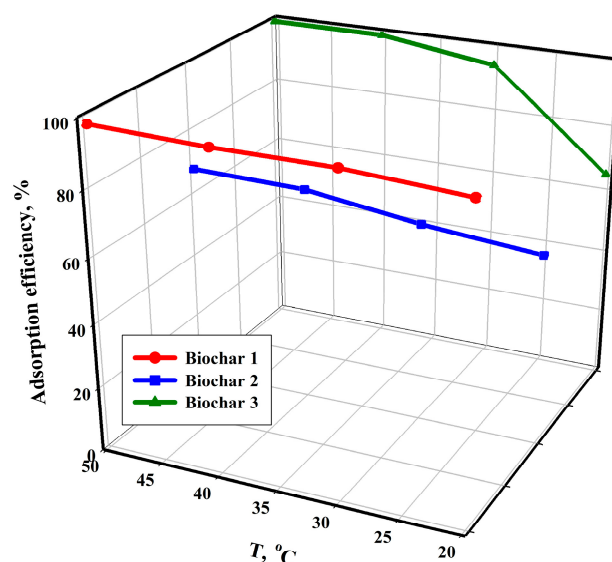


Figure 4. The influence of the temperature of the adsorption process on its efficiency ($t = 240$ (B1&B2), 120 (B3) min; $c = 100$ (B1), 200 (B2), 140 (B3) $\text{mg}\cdot\text{dm}^{-3}$; mass of adsorbent = 3.33 (B1), 1.67 (B2), 4 (B3) $\text{g}\cdot\text{dm}^{-3}$; $\text{pH} = 5$) [48–50].

The experimental data in Figure 5 show that the efficiency of the copper(II) cation adsorption process increases the most during the first two hours of contact between the adsorbent and the adsorbate for all studied sorbents. The equilibrium state in the tested systems is achieved relatively slowly. It is important to note that the time taken to reach equilibrium in the tested systems is not surprising. Previous research has shown that the adsorption of metal ions on carbon sorbents is slower than that on inorganic, hybrid or ion-exchange resins in terms of kinetics [78–81]. The initial increase in the efficiency of the copper(II) ion adsorption process can be attributed to the presence of numerous unsaturated adsorption sites and functional groups on the sorbent surface. As a result, there are more collisions on the surface of the studied sorbents between the Cu^{2+} cation and the active sites. The subsequent slow sorption is the result of the lower number of free sites and functional groups. The adsorption of Cu^{2+} cation on the studied sorbents is limited by two stages: mass transport and diffusion into the pores.

The kinetic models used during the study to describe the processes occurring on the surface of the tested sorbents showed that their nature is best described by a pseudo-second-order kinetic model [82,83]. On this basis, it should be assumed that the described adsorption processes are dominated by chemisorption, and limited by valent and covalent interactions. Based on the obtained values of k constants for the pseudo-second-order model—Table 5, it should be concluded that the adsorption process of the copper(II) ion with a concentration of $100 \text{ mg}\cdot\text{dm}^{-3}$ was the fastest on Biochar 3 and the slowest on Biochar 2.

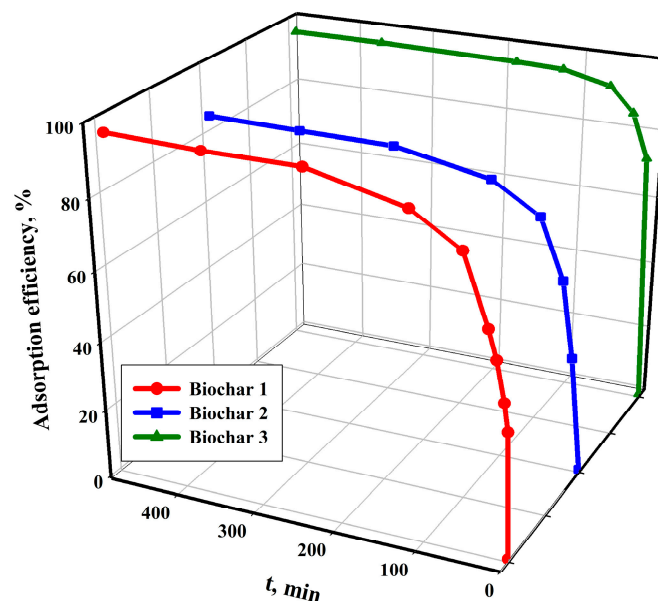


Figure 5. The influence of the contact time between the adsorbent and the adsorbate on the efficiency of the adsorption process ($T = 30\text{ }^{\circ}\text{C}$ (B1&B2), $20\text{ }^{\circ}\text{C}$ (B3); $c = 100$ (B1), 200 (B2), 50 (B3) $\text{mg}\cdot\text{dm}^{-3}$; mass of adsorbent = 3.33 (B1), 1.67 (B2), 6 (B3) $\text{g}\cdot\text{dm}^{-3}$; $\text{pH} = 5$) [48–50].

Table 5. Parameters for the adsorption of copper(II) ion on the studied biochars using the pseudo-second-order model [48–50].

Parameter	Biochar 1	Biochar 2	Biochar 3
$q_{e\text{ exp.}}, \text{mg}\cdot\text{g}^{-1}$	29.2	55.4	17.0
$q_{e\text{ cal.}}, \text{mg}\cdot\text{g}^{-1}$	29.6	58.3	17.2
$k, \text{g}\cdot\text{mg}^{-1}\cdot\text{min}^{-1}$	0.0050	0.0008	0.0414
R^2	0.999	0.999	0.999

Isotherm models were used to assess the adsorption capacity of adsorbents and determine sorption mechanisms. The Langmuir isotherm was found to provide the best description of the sorption mechanism on all studied sorbents. Langmuir's theory proposes that the adsorbate can form a monolayer of molecules that interact with adsorption sites through 'vertical' interactions, while not interacting or only weakly interacting with each other through 'horizontal' interactions. Adsorbate molecules in the liquid phase collide with the surface, and their probability of adsorption increases with the available free surface [84,85]. The data presented in Table 6 indicate that the studied sorbents have different surface structures. During the adsorption process, reactions mainly occur in the monolayer, without any other interactions that could cause multilayer adsorption effects.

Table 6. Calculated parameters of the Langmuir isotherm for the adsorption process of copper(II) ions on the studied biochars [48–50].

Parameter	Biochar 1	Biochar 2	Biochar 3
$q_m, \text{mg}\cdot\text{g}^{-1}$	52.2	90.4	37.7
$K, \text{dm}^3\cdot\text{mg}^{-1}$	0.360	0.149	0.382
R^2	0.999	0.999	0.999

The maximum sorption capacity, calculated based on the Langmuir isotherm, reached the highest value for Biochar 2: $90.4\text{ mg}\cdot\text{g}^{-1}$. Biochar 3 had the lowest sorption capacity: $37.7\text{ mg}\cdot\text{g}^{-1}$. This means that the modification of biochar with magnesium and sulphur oxides has a positive effect on the sorption properties of the material. The biochar surface

contains sulphur, resulting in the formation of several functional groups, such as sulphate and bisulphate. These groups have a positive impact on the Cu^{2+} cation sorption process occurring on the surface. The presence of $\text{Mg}(\text{OH})_2$ or MgO also has a positive impact on the adsorption process. The magnesium compounds have the ability to exchange or precipitate the copper(II) ion, thereby reducing its availability in waste acids. It is important to assume that the cation exchange mechanism plays a significant role in the adsorption processes on biochars [86,87].

It should be emphasised, however, that the sorption capacities of all the discussed sorbents was comparable to or much higher than those of similar materials of this type. Table 7 provides a summary of the maximum adsorption capacities obtained for the studied biochars in relation to the Cu^{2+} cation and the results obtained by other authors for various types of carbon sorbents.

Table 7. The capacity of various adsorbents to remove Cu^{2+} cation from aqueous solutions.

Adsorbent	q_m ($\text{mg}\cdot\text{g}^{-1}$)	Reference
Biochar 2	90.4	[49]
Biochar 1	52.2	[48]
Hydrochar	48.2	[88]
Manure biochar	44.5	[89]
Biochar 3	37.7	[50]
Activated carbon fibers	36.6	[90]
Sewage sludge biochar	25.6	[91]
Manure biochar	21.9	[76]
Hydroxylapatite-biochar	19.8	[92]
Miscanthus × Giganteus biochar	15.7	[93]
Rapeseed waste	15.4	[94]
Sunflowers husk biochar	13.2	[95]
Apple tree branches biochar	11.4	[96]
Paddy husk biochar	10.3	[97]
Hardwood biochar	4.39	[98]

Figure 6 represents a conceptual process flow sheet for the recovery of copper(II) from waste acidic liquids using a carbon sorbent obtained during the pyrolysis of waste rapeseed cake. It should be emphasised that the technological solution for waste rapeseed cake management proposed in the flow sheet eliminates potential threats related to the storage of the increasing amount of generated waste of this type and, above all, constitutes an alternative proposal for its management. The production of biochar from waste rapeseed cake in the pyrolysis process allows for liquid and gaseous fuels to be obtained for energy production, and the resulting biochar is a valuable carbon material for use in the recovery of valuable metals, such as copper, from technological streams. The saturated sorbent can be directed back to the metallurgical process as the equivalent of a part of coke being used together with copper concentrate as kiln input to the shaft furnace. This will also reduce the demand for coke used in the process. The proposed solution is attractive because the nearest prospects predict a further increase in copper demand in industry and the need to intensify recycling and recovery methods. It should also be emphasised that sustainable waste utilisation, including waste acids, is considered a preferred option to dumping or disposing of it untreated, in view of its potential economic and environmental benefits. Alternatively, the obtained biochar can be successfully used in agriculture and environmental protection. The application of biochar to agriculture may have a significant effect, reducing global warming through the reduction in greenhouse gas emissions. It may also have a significant effect on improving soil health and fertility. At the same time, biochar can help to sequester atmospheric carbon and purify drinking water [99,100].

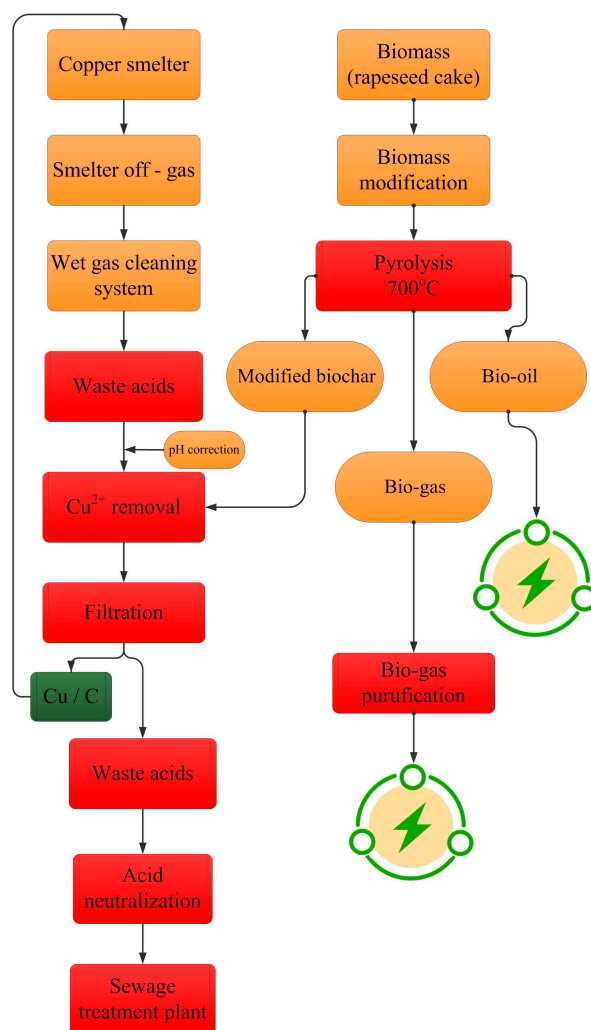


Figure 6. A conceptual flow diagram of the technological process of using biochar obtained from waste rapeseed cake for the recovery of copper(II) from technological streams.

6. Conclusions

This article describes the products and compares the sorption materials obtained from waste rapeseed cake through various modifications of the substrate. The study has shown that waste rapeseed cake can become a valuable raw material for obtaining highly efficient carbon sorbents for technological applications. The liquid and gaseous products obtained in the pyrolysis process can be successfully used in energy processes.

The presented results have proven that the waste modification method plays an important role in the sorption properties. The obtained sorbents are characterised by their high sorption capacity relative to the copper(II) ion, ranging from $40 \text{ mg}\cdot\text{g}^{-1}$ to $100 \text{ mg}\cdot\text{g}^{-1}$. Therefore, they can be successfully used for copper separation in the process of purifying waste technological acids. Moreover, owing to its relatively high combustion heat, the saturated sorbent can be used as a substitute for metallurgical coke.

The bio-gas derived from rapeseed cake primarily consists of carbon oxides, methane, and some volatile organic compounds. The concentration of carbon oxides in the gas decreases as the temperature increases, while the amount of methane that is produced increases. The gas obtained under high-temperature conditions, after the purification process, can be effectively used to generate heat or energy.

The bio-oil yield is relatively high and ranged around 55%. The analysis of bio-oil indicates that it is a carbon-rich oxy-fuel containing small amounts of nitrogen and sulphur. Bio-oil, with a significant combustion heat of $36 \text{ MJ}\cdot\text{kg}^{-1}$, can provide a source

of environmentally friendly green biofuel. Gasoline, diesel fuel, or alternative fractional products can be obtained through distillation or various processes, such as Fischer–Tropsch synthesis, cracking, and hydrogenation. These products can be used alone or blended with other conventional fuels.

Author Contributions: Conceptualization, K.M. and S.D.; methodology, K.M. and S.D.; validation, K.M., U.K. and B.I.; formal analysis, B.I., M.C. and A.W.-K.; investigation, K.M., A.W.-K. and S.D.; resources, U.K. and M.C.; data curation, K.M.; writing—original draft preparation, K.M.; writing—review and editing, S.D., U.K., M.C. and B.I.; visualization, K.M.; supervision, U.K.; project administration, K.M.; funding acquisition, U.K. All authors have read and agreed to the published version of the manuscript.

Funding: Nicolaus Copernicus University in Toruń.

Data Availability Statement: The authors confirm that the data supporting the findings of this study are available within the article.

Conflicts of Interest: Authors declare that they have no actual or potential conflicts of interest, including any financial, personal, or other relationships with other people or organisations, which could inappropriately influence their work.

References

1. Rico De La Hera, C. Special Issue on Biowaste Treatment and Valorization. *Appl. Sci.* **2022**, *12*, 11217. [CrossRef]
2. Ibanez, J.; Martel Martín, S.; Baldino, S.; Prandi, C.; Mannu, A. European Union Legislation Overview about Used Vegetable Oils Recycling: The Spanish and Italian Case Studies. *Processes* **2020**, *8*, 798. [CrossRef]
3. Montanarella, L.; Lugato, E. The Application of Biochar in the EU: Challenges and Opportunities. *Agronomy* **2013**, *3*, 462–473. [CrossRef]
4. Gonçalves, R.M.; Martinho, A.; Oliveira, J.P. Recycling of Reinforced Glass Fibers Waste: Current Status. *Materials* **2022**, *15*, 1596. [CrossRef]
5. Leppänen, T.; Mustonen, E.; Saarela, H.; Kuokkanen, M.; Tervonen, P. Productization of Industrial Side Streams into By-Products—Case: Fiber Sludge from Pulp and Paper Industry. *J. Open Innov. Technol. Mark. Complex.* **2020**, *6*, 185. [CrossRef]
6. Fan, Y.; Wu, S.; Lu, Y.; Zhao, Y. Study on the effect of the environmental protection industry and investment for the national economy: An input-output perspective. *J. Clean. Prod.* **2019**, *227*, 1093–1106. [CrossRef]
7. Kavanagh, J. Environmental protection and waste minimization: A case study. *J. Clean. Prod.* **1994**, *2*, 91–94. [CrossRef]
8. Fugiel, A.; Burchart-Korol, D.; Czaplicka-Kolarz, K.; Smoliński, A. Environmental impact and damage categories caused by air pollution emissions from mining and quarrying sectors of European countries. *J. Clean. Prod.* **2017**, *143*, 159–168. [CrossRef]
9. Statista. Available online: <https://www.statista.com/statistics/1245226/sulfuric-acid-market-volume-worldwide/> (accessed on 11 December 2023).
10. Grzesiak, P.; Grobela, M.; Motała, R. Ecological aspects and development strategies of sulfuric acid industry. *Przem. Chem.* **2013**, *92*, 1759–1764.
11. Grzesiak, P.; Grobela, M.; Motała, R.; Łukaszyc, J.; Schroeder, G.; Cichy, B. Strategy for dealing with waste materials in the production of sulfuric acid. *Przem. Chem.* **2011**, *90*, 1000–1004.
12. Grzesiak, P. Trend of sulfuric acid production in metallurgical installations. *Chemik* **2010**, *64*, 462–469.
13. Mazurek, K. Extraction of vanadium and potassium compounds from the spent vanadium catalyst from the metallurgical plant. *Pol. J. Chem. Technol.* **2012**, *14*, 49–53. [CrossRef]
14. King, M.J.; Davenport, W.G.; Moats, M.S. *Sulfuric Acid Manufacture*, 2nd ed.; Elsevier: Amsterdam, The Netherlands, 2013.
15. Grzesiak, P. *Development of Sulfuric Acid Production in Poland*; IOR: Poznań, Poland, 2004.
16. Rápó, E.; Tonk, S. Factors Affecting Synthetic Dye Adsorption; Desorption Studies: A Review of Results from the Last Five Years (2017–2021). *Molecules* **2021**, *26*, 5419. [CrossRef] [PubMed]
17. Younas, F.; Mustafa, A.; Farooqi, Z.U.R.; Wang, X.; Younas, S.; Mohy-Ud-Din, W.; Ashir Hameed, M.; Mohsin Abrar, M.; Maitlo, A.A.; Noreen, S.; et al. Current and Emerging Adsorbent Technologies for Wastewater Treatment: Trends, Limitations, and Environmental Implications. *Water* **2021**, *13*, 215. [CrossRef]
18. Quansah, J.O.; Hlaing, T.; Lyonga, F.N.; Kyi, P.P.; Hong, S.-H.; Lee, C.-G.; Park, S.-J. Nascent Rice Husk as an Adsorbent for Removing Cationic Dyes from Textile Wastewater. *Appl. Sci.* **2020**, *10*, 3437. [CrossRef]
19. Yousef, R.; Qiblawey, H.; El-Naas, M.H. Adsorption as a Process for Produced Water Treatment: A Review. *Processes* **2020**, *8*, 1657. [CrossRef]
20. Zamee, M.Z.A.; Sarjadi, M.S.; Rahman, M.L. Heavy Metals Removal from Water by Efficient Adsorbents. *Water* **2021**, *13*, 2659. [CrossRef]

21. Serban, G.V.; Iancu, V.I.; Dinu, C.; Tenea, A.; Vasilache, N.; Cristea, I.; Niculescu, M.; Ionescu, I.; Chiriac, F.L. Removal Efficiency and Adsorption Kinetics of Methyl Orange from Wastewater by Commercial Activated Carbon. *Sustainability* **2023**, *15*, 12939. [CrossRef]
22. Kuang, Y.; Zhang, X.; Zhou, S. Adsorption of Methylene Blue in Water onto Activated Carbon by Surfactant Modification. *Water* **2020**, *12*, 587. [CrossRef]
23. Xie, B.; Qin, J.; Wang, S.; Li, X.; Sun, H.; Chen, W. Adsorption of Phenol on Commercial Activated Carbons: Modelling and Interpretation. *Int. J. Environ. Res. Public Health* **2020**, *17*, 789. [CrossRef]
24. Okoniewska, E. Removal of Selected Dyes on Activated Carbons. *Sustainability* **2021**, *13*, 4300. [CrossRef]
25. Lach, J.; Ociepa-Kubicka, A.; Mrowiec, M. Oxytetracycline Adsorption from Aqueous Solutions on Commercial and High-Temperature Modified Activated Carbons. *Energies* **2021**, *14*, 3481. [CrossRef]
26. Rivera-Utrilla, J.; Sánchez-Polo, M.; Gómez-Serrano, V.; Álvarez, P.M.; Alvim-Ferraz, M.C.M.; Dias, J.M. Activated carbon modifications to enhance its water treatment applications. An overview. *J. Hazard. Mater.* **2011**, *187*, 1–23. [CrossRef] [PubMed]
27. Tauetsile, P.J.; Oraby, E.A.; Eksteen, J.J. Adsorption behaviour of copper and gold Glycinates in alkaline media onto activated carbon. Part 2: Kinetics. *Hydrometallurgy* **2018**, *178*, 195–201. [CrossRef]
28. Foong, S.Y.; Liew, R.K.; Yang, Y.; Cheng, Y.W.; Wan Mahari, W.A.; Peng, W.; Lam, S.S. Valorization of biomass waste to engineered activated biochar by microwave pyrolysis: Progress, challenges, and future directions. *Chem. Eng. J.* **2020**, *389*, 124401. [CrossRef]
29. Nie, T.; Yang, X.; Chen, H.; Muller, K.; Shaheen, S.M.; Rinklebe, J.; Song, H.; Xu, S.; Wu, F.; Wang, H. Effect of biochar aging and co-existence of diethyl phthalate on the mono-sorption of cadmium and zinc to biochar-treated soils. *J. Hazard. Mater.* **2021**, *408*, 124850. [CrossRef]
30. Wang, J.; Wang, S. Preparation, modification and environmental application of biochar: A review. *J. Clean. Prod.* **2021**, *227*, 1002–1022. [CrossRef]
31. Kang, Z.; Jia, X.; Zhang, Y.; Kang, X.; Ge, M.; Liu, D.; Wang, C.; He, Z. A Review on Application of Biochar in the Removal of Pharmaceutical Pollutants through Adsorption and Persulfate-Based AOPs. *Sustainability* **2022**, *14*, 10128. [CrossRef]
32. Sun, Y.; Yu, F.; Han, C.; Houda, C.; Hao, M.; Wang, Q. Research Progress on Adsorption of Arsenic from Water by Modified Biochar and Its Mechanism: A Review. *Water* **2022**, *14*, 1691. [CrossRef]
33. Shi, Z.; Ma, A.; Chen, Y.; Zhang, M.; Zhang, Y.; Zhou, N.; Fan, S.; Wang, Y. The Removal of Tetracycline from Aqueous Solutions Using Peanut Shell Biochars Prepared at Different Pyrolysis Temperatures. *Sustainability* **2023**, *15*, 874. [CrossRef]
34. Wang, C.; Wang, X.; Li, N.; Tao, J.; Yan, B.; Cui, X.; Chen, G. Adsorption of Lead from Aqueous Solution by Biochar: A Review. *Clean Technol.* **2022**, *4*, 629–652. [CrossRef]
35. Chatzimichailidou, S.; Xanthopoulou, M.; Tolkou, A.K.; Katsoyiannis, I.A. Biochar Derived from Rice by-Products for Arsenic and Chromium Removal by Adsorption: A Review. *J. Compos. Sci.* **2023**, *7*, 59. [CrossRef]
36. Wang, Y.; Li, H.; Lin, S. Advances in the Study of Heavy Metal Adsorption from Water and Soil by Modified Biochar. *Water* **2022**, *14*, 3894. [CrossRef]
37. Dygas, D.; Liszkowska, W.; Steglińska, A.; Sulyok, M.; Kręgiel, D.; Berłowska, J. Rapeseed Meal Waste Biomass as a Single-Cell Protein Substrate for Nutritionally-Enhanced Feed Components. *Processes* **2023**, *11*, 1556. [CrossRef]
38. Rakita, S.; Kokić, B.; Manoni, M.; Mazzoleni, S.; Lin, P.; Luciano, A.; Ottoboni, M.; Cheli, F.; Pinotti, L. Cold-Pressed Oilseed Cakes as Alternative and Sustainable Feed Ingredients: A Review. *Foods* **2023**, *12*, 432. [CrossRef] [PubMed]
39. Paciorek-Sadowska, J.; Borowicz, M.; Isbrandt, M.; Czupryński, B.; Apiecionek, Ł. The Use of Waste from the Production of Rapeseed Oil for Obtaining of New Polyurethane Composites. *Polymers* **2019**, *11*, 1431. [CrossRef] [PubMed]
40. Di Lena, G.; Sanchez del Pulgar, J.; Lucarini, M.; Durazzo, A.; Ondrejčková, P.; Oancea, F.; Frincu, R.-M.; Aguzzi, A.; Ferrari Nicoli, S.; Casini, I.; et al. Valorization Potentials of Rapeseed Meal in a Biorefinery Perspective: Focus on Nutritional and Bioactive Components. *Molecules* **2021**, *26*, 6787. [CrossRef]
41. Zheng, Q.; Liu, K. Worldwide rapeseed (*Brassica napus* L.) research: A bibliometric analysis during 2011–2021. *Oil Crop Sci.* **2021**, *7*, 157–165. [CrossRef]
42. Jannat, A.; Ishikawa-Ishiwata, Y.; Furuya, J. Does Climate Change Affect Rapeseed Production in Exporting and Importing Countries? Evidence from Market Dynamics Syntheses. *Sustainability* **2022**, *14*, 6051. [CrossRef]
43. Statista. Available online: <https://www.statista.com/statistics/263930/worldwide-production-of-rapeseed-by-country/> (accessed on 11 December 2023).
44. Gallorini, R.; Aquilia, S.; Bello, C.; Ciardelli, F.; Pinna, M.; Papini, A.; Rosi, L. Pyrolysis of spent rapeseed meal: A circular economy example for waste valorization. *J. Anal. Appl. Pyrolysis* **2023**, *174*, 106138. [CrossRef]
45. Raboanatahiry, N.; Li, H.; Yu, L.; Li, M. Rapeseed (*Brassica napus*): Processing, Utilization, and Genetic Improvement. *Agronomy* **2021**, *11*, 1776. [CrossRef]
46. So, K.K.Y.; Duncan, R.W. Breeding Canola (*Brassica napus* L.) for Protein in Feed and Food. *Plants* **2021**, *10*, 2220. [CrossRef] [PubMed]
47. Tileuberdi, N.; Turgumbayeva, A.; Yeskaliyeva, B.; Sarsenova, L.; Issayeva, R. Extraction, Isolation of Bioactive Compounds and Therapeutic Potential of Rapeseed (*Brassica napus* L.). *Molecules* **2022**, *27*, 8824. [CrossRef] [PubMed]
48. Mazurek, K.; Drużyński, S.; Kiełkowska, U.; Szłyk, E. New separation material obtained from waste rapeseed cake for copper(II) and zinc(II) removal from the industrial wastewater. *Materials* **2021**, *14*, 2566. [CrossRef]

49. Mazurek, K.; Drużyński, S.; Kielkowska, U.; Bielicka, A.; Glużyńska, J. Application of sulphate and magnesium enriched waste rapeseed cake biochar for recovery of Cu(II) and Zn(II) from industrial wastewater generated in sulphuric acid plants. *Hydrometallurgy* **2023**, *216*, 106014. [[CrossRef](#)]
50. Drużyński, S.; Mazurek, K.; Kielkowska, U.; Wróbel-Kaszanek, A.; Igliński, B. Physicochemical Properties and Application of Silica-Doped Biochar Composites as Efficient Sorbents of Copper from Tap Water. *Materials* **2023**, *16*, 2794. [[CrossRef](#)]
51. Singer, D.A. Future copper resources. *Ore Geol. Rev.* **2017**, *86*, 271–279. [[CrossRef](#)]
52. Kuipers, K.; van Oers, L.; Verboon, M.; van der Voet, E. Assessing environmental implications associated with global copper demand and supply scenarios from 2010 to 2050. *Glob. Environ. Chang.* **2018**, *49*, 106–115. [[CrossRef](#)]
53. Ucar, S.; Ozkan, A. Characterization of products from the pyrolysis of rapeseed oil cake. *Bioresour. Technol.* **2008**, *99*, 8771–8776. [[CrossRef](#)]
54. Atelge, M.R.; Senol, H.; Djaafri, M.; Hansu, T.A.; Krisa, D.; Atabani, A.; Eskicioglu, C.; Muratçobanoğlu, H.; Unalan, S.; Kalloum, S.; et al. A Critical Overview of the State-of-the-Art Methods for Biogas Purification and Utilization Processes. *Sustainability* **2021**, *13*, 11515. [[CrossRef](#)]
55. Adnan, A.I.; Ong, M.Y.; Nomanbhay, S.; Chew, K.W.; Show, P.L. Technologies for Biogas Upgrading to Biomethane: A Review. *Bioengineering* **2019**, *6*, 92. [[CrossRef](#)]
56. Papurello, D.; Gandiglio, M.; Kafashan, J.; Lanzini, A. Biogas Purification: A Comparison of Adsorption Performance in D4 Siloxane Removal Between Commercial Activated Carbons and Waste Wood-Derived Char Using Isotherm Equations. *Processes* **2019**, *7*, 774. [[CrossRef](#)]
57. Guo, P.; Zhang, Y.; Zhao, Y. Biocapture of CO₂ by Different Microalgal-Based Technologies for Biogas Upgrading and Simultaneous Biogas Slurry Purification under Various Light Intensities and Photoperiods. *Int. J. Environ. Res. Public Health* **2018**, *15*, 528. [[CrossRef](#)]
58. Sethupathi, S.; Zhang, M.; Rajapaksha, A.U.; Lee, S.R.; Mohamad Nor, N.; Mohamed, A.R.; Al-Wabel, M.; Lee, S.S.; Ok, Y.S. Biochars as Potential Adsorbers of CH₄, CO₂ and H₂S. *Sustainability* **2017**, *9*, 121. [[CrossRef](#)]
59. Ozcimen, D.; Karaosmanoglu, F. Production and characterization of bio-oil and biochar from rapeseed cake. *Renew. Energy* **2004**, *29*, 779–787. [[CrossRef](#)]
60. Shang, H.; Li, Y.; Liu, J.; Wan, Y.; Yu, Y.L. Preparation of nitrogen doped magnesium oxide modified biochar and its sorption efficiency of lead ions in aqueous solution. *Bioresour. Technol.* **2020**, *314*, 123708. [[CrossRef](#)]
61. Ling, L.L.; Liu, W.J.; Zhang, S.; Hong, J. Magnesium oxide embedded nitrogen self-doped biochar composites: Fast and high-efficiency adsorption of heavy metals in an aqueous solution. *Environ. Sci. Technol.* **2017**, *51*, 10081–10089. [[CrossRef](#)]
62. Jellali, S.; Diamantopoulos, E.; Haddad, K.; Anane, M.; Durner, W.; Mlayah, A. Lead removal from aqueous solutions by raw sawdust and magnesium pretreated biochar: Experimental investigations and numerical modelling. *J. Environ. Manag.* **2016**, *180*, 439–449. [[CrossRef](#)]
63. Yin, G.; Tao, L.; Chen, X.; Bolan, N.S.; Sarkar, B.; Lin, Q.; Wang, H. Quantitative analysis on the mechanism of Cd²⁺ removal by MgCl₂-modified biochar in aqueous solutions. *J. Hazard. Mater.* **2021**, *420*, 126487. [[CrossRef](#)]
64. Zhang, J.; Hou, D.; Shen, Z.; Jin, F.; O'Connor, D.; Pan, S.; Ok, Y.S.; Tsang, D.; Bolan, N.S.; Alessi, D.S. Effects of excessive impregnation, magnesium content, and pyrolysis temperature on MgO-coated watermelon rind biochar and its lead removal capacity. *Environ. Res.* **2020**, *183*, 109152. [[CrossRef](#)]
65. Cheng, S.; Zhao, S.; Guo, H.; Xing, B.; Liu, Y.; Zhang, C.; Ma, M. High-efficiency removal of lead/cadmium from wastewater by MgO modified biochar derived from crofton weed. *Bioresour. Technol.* **2022**, *343*, 126081. [[CrossRef](#)]
66. Li, R.; Wang, J.J.; Zhou, B.; Awasthi, M.K.; Ali, A.; Zhang, Z.; Lahori, A.H.; Mahar, A. Recovery of phosphate from aqueous solution by magnesium oxide decorated magnetic biochar and its potential as phosphate-based fertilizer substitute. *Bioresour. Technol.* **2016**, *215*, 209–214. [[CrossRef](#)]
67. Wang, P.; Zhan, S.; Yu, H.; Xue, X.; Hong, N. The effects of temperature and catalysts on the pyrolysis of industrial wastes (herb residue). *Bioresour. Technol.* **2018**, *101*, 3236–3241. [[CrossRef](#)]
68. Lee, M.-E.; Park, J.H.; Chung, J.W. Adsorption of Pb(II) and Cu(II) by Ginkgo-Leaf-Derived Biochar Produced under Various Carbonization Temperatures and Times. *Int. J. Environ. Res. Public Health* **2017**, *14*, 1528. [[CrossRef](#)]
69. Kim, B.S.; Lee, H.W.; Park, S.H.; Baek, K.; Jeon, J.; Cho, H.J.; Jung, S.; Kim, S.C.; Park, Y. Removal of Cu²⁺ by biochars derived from green macroalgae. *Environ. Sci. Pollut. Res.* **2016**, *23*, 985–994. [[CrossRef](#)]
70. Khandaker, S.; Hossain, T.; Saha, P.; Rayhan, U.; Islam, A.; Choudhury, T.; Awwal, M.R. Functionalized layered double hydroxides composite bio-adsorbent for efficient copper(II) ion encapsulation from wastewater. *J. Environ. Manag.* **2021**, *300*, 113782. [[CrossRef](#)]
71. Zhang, P.; Zhang, X.; Yuan, X.; Xie, R.; Han, L. Characteristics, adsorption behaviors, Cu(II) adsorption mechanisms by cow manure biochar derived at various pyrolysis temperatures. *Bioresour. Technol.* **2021**, *331*, 125013. [[CrossRef](#)]
72. Katiyar, R.; Patel, A.K.; Nguyen, T.; Singhania, R.R.; Chen, C.; Dong, C. Adsorption of copper(II) in aqueous solution using biochars derived from *Ascophyllum nodosum* seaweed. *Bioresour. Technol.* **2021**, *328*, 124829. [[CrossRef](#)]
73. Chen, Y.; Li, M.; Li, Y.; Liu, Y.; Chen, Y.; Li, H.; Li, L.; Xu, F.; Jiang, H.; Chen, L. Hydroxyapatite modified sludge-based biochar for the adsorption of Cu²⁺ and Cd²⁺: Adsorption behavior and mechanisms. *Bioresour. Technol.* **2021**, *321*, 124413. [[CrossRef](#)]

74. Znad, H.; Awual, M.R.; Martini, S. The Utilization of Algae and Seaweed Biomass for Bioremediation of Heavy Metal-Contaminated Wastewater. *Molecules* **2022**, *27*, 1275. [[CrossRef](#)]
75. Liu, Z.; Zhang, F. Removal of lead from water using biochars prepared from hydrothermally liquefaction of biomass. *J. Hazard. Mater.* **2009**, *167*, 933–939. [[CrossRef](#)]
76. Meng, J.; Feng, X.; Dai, Z.; Liu, X.; Wu, J.; Xu, J. Adsorption characteristics of Cu(II) from aqueous solution onto biochar derived from swine manure. *Environ. Sci. Pollut. Res.* **2014**, *21*, 7035–7046. [[CrossRef](#)]
77. Mazurek, K.; Weidner, E.; Drużyński, S.; Ciesielczyk, F.; Kielkowska, U.; Wróbel-Kaszanek, A.; Jesionowski, T. Lanthanum enriched TiO₂-ZrO₂ hybrid material with tailored physicochemical properties dedicated to separation of lithium and cobalt(II) raising from the hydrometallurgical stage of the recycling process of lithium ion batteries. *Hydrometallurgy* **2020**, *197*, 105448. [[CrossRef](#)]
78. Li, Q.; Fu, L.; Wang, Z.; Li, A.; Shuang, C.; Gao, C. Synthesis and characterization of a novel magnetic cation exchange resin and its application for efficient removal of Cu²⁺ and Ni²⁺ from aqueous solutions. *J. Clean. Prod.* **2017**, *165*, 801–810. [[CrossRef](#)]
79. Maleki, A.; Hajizadeh, Z.; Sharifi, V.; Embadi, Z. A green, porous and eco-friendly magnetic geopolymer adsorbent for heavy metals removal from aqueous solutions. *J. Clean. Prod.* **2019**, *215*, 1233–1245. [[CrossRef](#)]
80. Awual, M.R.; Yaita, T.; Okamoto, Y. A novel ligand based dual conjugate adsorbent for cobalt(II) and copper(II) ions capturing from water. *Sens. Actuators B* **2014**, *203*, 71–80. [[CrossRef](#)]
81. Bouhamed, F.; Elouear, Z.; Bouzid, J.; Ouddane, B. Multi-component adsorption of copper, nickel and zinc from aqueous solutions onto activated carbon prepared from date stones. *Environ. Sci. Pollut. Res.* **2015**, *23*, 15801–15806. [[CrossRef](#)]
82. Ho, Y.S.; McKay, G. Pseudo-second order model for sorption processes. *Process Biochem.* **1999**, *34*, 451–465. [[CrossRef](#)]
83. Nyamunda, B.C.; Chivhanga, T.; Guyo, U.; Chigondo, F. Removal of Zn(II) and Cu(II) Ions from Industrial Wastewaters Using Magnetic Biochar Derived from Water Hyacinth. *J. Eng.* **2019**, *2019*, 5656983. [[CrossRef](#)]
84. Chen, X. Modeling of Experimental Adsorption Isotherm Data. *Information* **2015**, *6*, 14–22. [[CrossRef](#)]
85. Sulaiman, N.S.; Mohamad Amini, M.H.; Danish, M.; Sulaiman, O.; Hashim, R. Kinetics, Thermodynamics, and Isotherms of Methylene Blue Adsorption Study onto Cassava Stem Activated Carbon. *Water* **2021**, *13*, 2936. [[CrossRef](#)]
86. Park, J.H.; Wang, J.J.; Kim, S.H.; Cho, J.S.; Kang, S.W.; Delaune, R.D.; Han, K.J.; Seo, D.C. Recycling of rice straw through pyrolysis and its adsorption behaviors for Cu and Zn ions in aqueous solution. *Colloids Surf. A* **2017**, *533*, 330–337. [[CrossRef](#)]
87. Lu, H.; Zhang, W.; Yang, Y.; Huang, X.; Wang, S.; Qiu, R. Relative distribution of Pb²⁺ sorption mechanisms by sludge-derived biochar. *Water Res.* **2012**, *46*, 854–862. [[CrossRef](#)]
88. Semercioz, A.S.; Gogus, F.; Celekli, A.; Bozkurt, H. Development of carbonaceous material from grapefruit peel with microwave implemented-low temperature hydrothermal carbonization technique for the adsorption of Cu(II). *J. Clean. Prod.* **2017**, *165*, 599–610. [[CrossRef](#)]
89. Idrees, M.; Batool, S.; Kalsoom, T.; Yasmeen, S.; Kalsoom, A.; Raina, S.; Zhuang, Q.; Kong, J. Animal manure-derived biochars produced via fast pyrolysis for the removal of divalent copper from aqueous media. *J. Environ. Manag.* **2018**, *213*, 109–118. [[CrossRef](#)]
90. Qiao, K.; Yu, J.; Zhu, B.; Chi, C.; Di, C.; Cheng, Y.; Shang, M.; Li, C. Oxygen-Rich Activated Carbon Fibers with Exceptional Cu(II) Adsorptivity and Recycling Performance. *Ind. Eng. Chem. Res.* **2020**, *59*, 13088–13094. [[CrossRef](#)]
91. Mazurek, K.; Drużyński, S.; Kielkowska, U.; Węgrzynowicz, A.; Nowak, A.K.; Wzorek, Z.; Wróbel-Kaszanek, A. Municipal Sewage Sludge as a Source for Obtaining Efficient Biosorbents: Analysis of Pyrolysis Products and Adsorption Tests. *Materials* **2023**, *16*, 2648. [[CrossRef](#)]
92. Cen, Y.; Li, Y.; Deng, H.; Ding, H.; Tang, S.; Yu, X.; Xu, F.; Zhu, Z.; Zhu, Y. Removal of Copper (II) from Aqueous Solution by a Hierarchical Porous Hydroxylapatite-Biochar Composite Prepared with Sugarcane Top Internode Biotemplate. *Water* **2022**, *14*, 839. [[CrossRef](#)]
93. Cibati, A.; Foereid, B.; Bissessur, A.; Hapca, S. Assessment of Miscanthus × Giganteus Derived Biochar as Copper and Zinc adsorbent: Study of the Effect of Pyrolysis Temperature, pH and Hydrogen Peroxide Modification. *J. Clean. Prod.* **2017**, *162*, 1285–1296. [[CrossRef](#)]
94. Tofan, L.; Paduraru, C.; Volf, I.; Toma, O. Waste of Rapeseed from Biodiesel Production as a Potential Biosorbent for Heavy Metal Ions. *BioResorces* **2011**, *6*, 3727–3741. [[CrossRef](#)]
95. Tomczyk, A.; Sokołowska, Z.; Boguta, P. Biomass type effect on biochar surface characteristic and adsorption capacity relative to silver and copper. *Fuel* **2020**, *278*, 118168. [[CrossRef](#)]
96. Zhao, S.; Ta, N.; Wang, X. Absorption of Cu(II) and Zn(II) from Aqueous Solutions onto Biochars Derived from Apple Tree Branches. *Energies* **2020**, *13*, 3498. [[CrossRef](#)]
97. Wijeyawardana, P.; Nanayakkara, N.; Gunasekara, C.; Karunarathna, A.; Law, D.; Pramanik, B. Removal of Cu, Pb and Zn from stormwater using an industrially manufactured sawdust and paddy husk derived biochar. *Environ. Technol. Innov.* **2022**, *28*, 102640. [[CrossRef](#)]
98. Jiang, S.; Huang, L.; Nguyen, T.A.; Ok, Y.S.; Rudolph, V.; Yang, H.; Zhang, D. Copper and Zinc Adsorption by Softwood and Hardwood Biochars under Elevated Sulphate-Induced Salinity and Acidic pH Conditions. *Chemosphere* **2016**, *142*, 64–71. [[CrossRef](#)]

99. Li, X.; Huang, Z.; Shao, S.; Cai, Y. Machine learning prediction of physical properties and nitrogen content of porous carbon from agricultural wastes: Effects of activation and doping process. *Fuel* **2024**, *356*, 129623. [[CrossRef](#)]
100. Shao, S.; Wang, Y.; Ma, L.; Huang, Z.; Li, X. Sustainable preparation of hierarchical porous carbon from discarded shells of crustaceans for efficient CO₂ capture. *Fuel* **2024**, *355*, 129287. [[CrossRef](#)]

Disclaimer/Publisher's Note: The statements, opinions and data contained in all publications are solely those of the individual author(s) and contributor(s) and not of MDPI and/or the editor(s). MDPI and/or the editor(s) disclaim responsibility for any injury to people or property resulting from any ideas, methods, instructions or products referred to in the content.